UNIVERSIDAD DEL ZULIA
Serbiluz Sistema de Servicios Bibliotecarios y de Información
Biblioteca Digital Repositorio Académico

Invest Clin 61(2): 600-608, 2020

Fully Automatic Ultrasound Fetal Heart Image Detection and Segmentation based on Texture Analysis

Chunlin Song
State Key Laboratory of Software Development Environment, Beihang University, Beijing, China
BOE Technology Group Co. Ltd, Beijing, China

Tao Gao
Obstetrics & Gynecology, Wuxi People's Hospital, Wuxi, Jiangsu, China

Yuxin Gong
State Key Laboratory of Software Development Environment, Beihang University, Beijing, China

Sud Sudirman
Department of Computer Science, Liverpool John Moores University, Liverpool, UK

Hong Wang
BOE Technology Group Co.Ltd, Beijing, China

Haogang Zhu*
State Key Laboratory of Software Development Environment, Beihang University, Beijing, China
Corresponding author (E-mail: haogangzhu@buaa.edu.cn)

Abstract
Ultrasound fetal heart image analysis is important for the antenatal diagnosis of congenital heart disease, therefore, design an automated fetal heart ultrasound image analysis approaches to improve detection ratio of congenital heart disease is necessary. Nevertheless, because of the complicated structure of fetal heart ultrasound image, location, detection and segmentation approaches of fetal heart images as interesting topics that get more attention. Therefore, in this work, we present a framework to segment ultrasound image automatically for tracking the boundary of fetal heart region. In the first step, this paper contributes to breed candidate regions. And then, in the segmentation progress, we apply an energy-based active contour model to detect the edges of fetal heart. Finally, in the experiment section, the performance is estimated by the Dice similarity coefficient, which calculate the spatial overlap between two different segmentation regions, and the experiment results indicate that the proposed algorithm achieves high levels of accuracy.

Key words: Ultrasound Image Analyze, Fetal Heart, Region of Interest, Image Segmentation, Gradient Vector Flow

1. Introduction

Congenital heart disease is one of the most common defects at birth which covers several specific problems to detect the normal and abnormal structure of fetal heart. An investigation report indicated that, more than 82% of major congenital heart diseases were not detected during the processing of pregnancy examination [1], the detection rates are heavily dependent on the number of factors such as training of the sonographer, the nature of the defection and a variety of different viewing planes includes four-chamber (4C) view plane, the left ventricular outflow tract (LVOT) and three vessels (3V) view which is shown in Fig.1 [2].

Computer-aided diagnosis (CAD) system based on B-mode fetal ultrasound is an important and standard manner which has been developed to distinguish the congenital heart disease, it has been clinically tested their ability to improve the performance of the fetal abnormalities diagnosis due to its relative safety, noninvasive, nonradioactive, cost-effective, real-time display, operator comfort, operator experience and lack of harmful for fetus and mother [2]. Fetal ultrasound image technology has rapid developed and it becomes the primary screening modality for pregnancy evaluation. Therefore, to design and develop pattern recognition algorithm to facilities obstetrical ultrasound image of fetal heart is important to increase detection rates of congenital heart disease and reduce associated perinatal morbidity and mortality.

UNIVERSIDAD DEL ZULIA
Serbiluz
Sistema de Servicios Bibliotecarios y de Información
Biblioteca Digital
Repositorio Académico

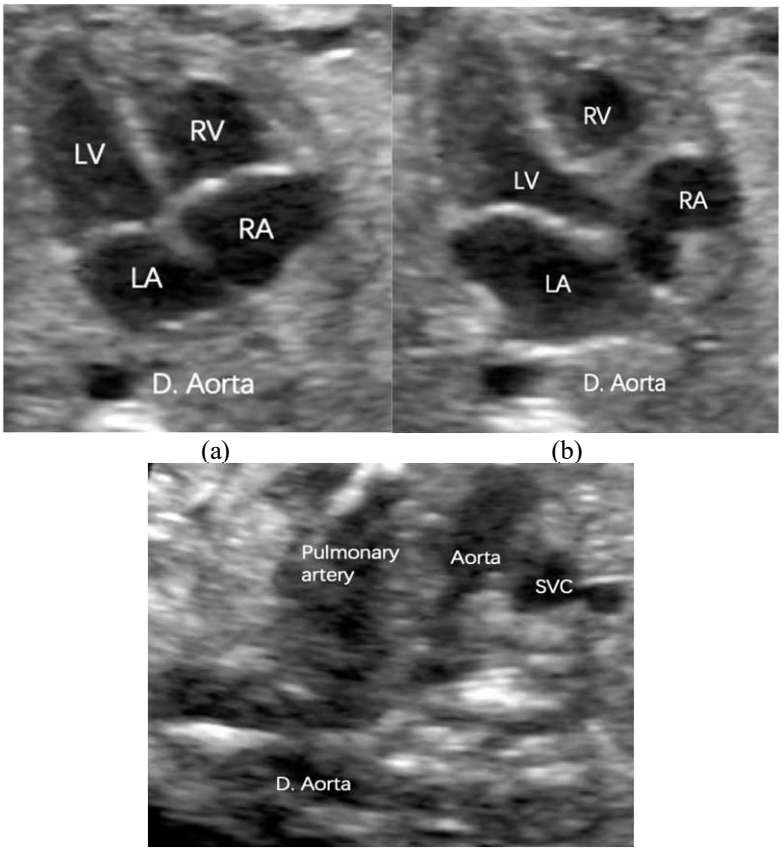

Figure 1. (a) Four-chamber view; (b) the left ventricular outflow tract view; (c) three vessel view. LV and RV are described as left and right ventricle; LA and RA are defined as left and right atrium; D. Aorta, descending aorta; SVC, superior vena cava

Analysis four chamber viewing plane is one of the most useful procedures and have been widely used in the diagnosis of congenital heart disease which serves for detecting abnormalities throughout gestation. However, it faces numbers of challenging problems due to a variety of reasons. First of all, the complicated image characteristic such as attenuation, speckle, shadow, signal dropout makes the analysis difficulty. Secondly, the fetal heart has complicated shapes and appearance, their pattern can vary from weeks to weeks, and differs from patient to patient.

The previous works have been carried out towards above aim. In [3], the author proposed the Transverse Dyadic Wavelet Transform algorithm to preserve the border and curvature of four chambers from 18 to 22 weeks ultrasound fetal heart image. Another paper is described in [4] proposed a spatially constrained-distance regularized level set evolution segmentation algorithm to identify hydrops fetalis from ultrasound fetal heart images. Seridevi proposed a fuzzy-connectedness based approach, it involved probabilistic patch based maximum likelihood estimation as the denoising technique, and applied Fuzzy connectedness technique to segment fetal heart image [32]. Erik in [33] published a deep learning-based approach for segmenting left ventricle in ultrasound fetal heart images. In addition, Christopher proposed an algorithm to predict visibility, location and orientation of the fetal heart ultrasound image from each frame at ultrasound videos [2].

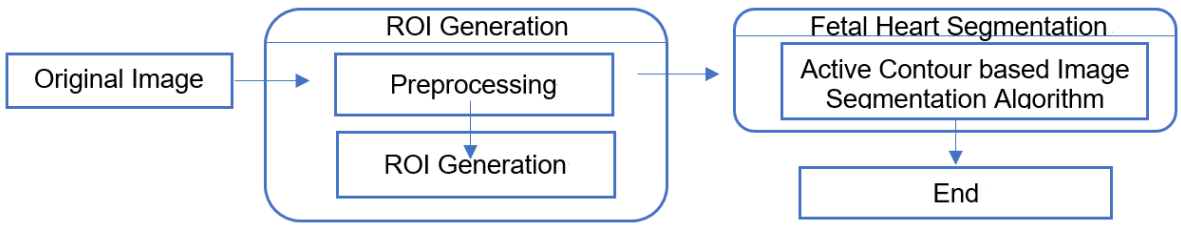

Figure 2. The flow-chart of the recommended algorithm

UNIVERSIDAD DEL ZULIA
Serbiluz
Sistema de Servicios Bibliotecarios y de Información
Biblioteca Digital
Repositorio Académico

Although the previous work introduces several schemes for analyzing fetal heart ultrasound images, however, the active contour-based algorithm has a great development prospect [34], it provides another solution in this field. Therefore, in this paper, we investigate the typical problem of automatically segmenting healthy and unhealthy ultrasound fetal heart image. The two-step strategy is introduced in this paper: first of all, the fetal heart location is positioned as the region of interests (ROI) and then the features and characteristic have segmented from the ROIs. The flow-chart of the recommended algorithm is shown in Fig.2.

The outline of this paper is planned as follows. The fully automatic ROI generation algorithm is described in section 2. After that, the segmentation algorithm is discussed in section 3, then in section 4, the experiment and the results are explained. The final section discusses the characteristic of the proposed algorithm, concludes the entire work and directs the future.

2. ROI Generation

The process of ROI generation is the precondition stage for automatic segmentation and classification of fetal heart. The ROIs function as a user-defined indicator in regular shape of the scene in most of the times for supporting the perception task. A rectangular region as a usual mold which delivers the location of fetal heart and excludes the rest of tissues as much as possible. The following characteristics of an ideal ROI generation approaches are described:

(1) Fully automatic: the proposed generation algorithm should avoid manual and semi-automatic approaches

(2) The region of fetal heart coverage completely: Ideally, a ROI-generation algorithm would complete cover the fetal heart and exclude normal regions as much as possible for achieving high segmentation accuracy.

2.1. Preprocessing

In the 2D ultrasound images, the fetal heart appears relatively darker comparing with the neighboring tissues due to the low-level echo reflection. However, due to the complexity environment of ultrasound images, the ultrasound fetal heart images always have low level quality caused by speckle noise, low-contrast and shadow effect. In addition, due to the reliability of operator-dependent and the facts of device-dependent, the gray-level contrast and textures in different images vary greatly. Therefore, the preprocessing is focused on enhancing the hypoechoic regions, normalizing intensities and reducing noise. The following steps are listed below:

Smoothing: a two-dimension low pass Gaussian filter is applied to ultrasound images to reduce noise in the frequency domain.

Normalization: the enhanced image I_b is produced through the fuzzy domain algorithm [5] from the gray level of smoothing image. Z-shaped function is illustrated as Eq. (1) which is applied to gray scale smoothing image by transforming the intensities from [0, 1].

$$Z(x_i,a,b,c)=\begin{cases}1 & if\ x_i\le a\\ 1-\frac{(x_i-a)^2}{(c-a)(b-a)} & if a<x_i<b\\ \frac{(I(x)-c)^2}{(c-a)(b-a)} & if b<x_i<c\\ 0 & if\ otherwise\end{cases} \tag{1}$$

In Eq. (1), the factors a and c are determined by the nonlinear range of the curve which is defined as 1 and 32 respectively, b is determined as Eq.(2) which is devoted to adjust the steepness of the curve. It is decided adaptively in terms of the skewness of the intensity distribution.

$$b=\begin{cases}\frac{a+c}{2} & if\ SN\le 0\\ \frac{a+c(1-SN)}{2} & if\ SN>0\end{cases} \tag{2}$$

$$SN=\frac{\sqrt{(n-1)(n-2)}}{n}\frac{1/n\sum_{i=1}^{n}(x_i-\bar{x})^3}{[1/n\sum_{i=1}^{n}(x_i-\bar{x})^2]^{3/2}} \tag{3}$$

Eq. (3) is the bias-corrected skewness statistic algorithm [6] to measure the asymmetry of the image intensity distribution. It represents the larger the skewness becomes, the more and the mass of the distribution concentrates on the left side. In addition, in the above equations, x_i is the intensity of the i^{th} pixel, $\bar{x}$ denotes the mean of image intensities and n represents the number of pixel.

2.2. ROI Generation

After the pre-processing phase, the next step is constructed ROI. The following stages of ROI generation is listed below:

UNIVERSIDAD DEL ZULIA Serbiluz Sistema de Servicios Bibliotecarios y de Información Biblioteca Digital Repositorio Académico

(1) Find connected components: connected components labelling works on gray-level fetal heart image in order to measure and identify connected pixel regions based on pixel connectivity [7]. Therefore, in this step, we will find all the connected components in enhanced gray scale image I_b, each connected component signifies a possible fetal heart region after all the components are found. The real fetal heart region is always located at the center of the image. In other words, the boundary regions do not in the center position would be considered as 'fake' region. Therefore, the 'fake' regions are removed from the candidate list.

(2) Rank the potential regions: the rest of the connected components of enhanced gray-level image would be ranked through the Eq.(4).

$$S_n = \frac{\sqrt{Area_n}}{dis(C_n, C_0)} \qquad n = 1, \dots, k \tag{4}$$

Where k and $Area_n$ represent as the number of candidate regions and the number of pixels in the region, respectively. C_n and C_0 denote the center of the region and image, the last label dis(C_n, C_0) is represented as Euclidean distance between points C_n and C_0. The one with the highest values is recognized as the original fetal heart region ROI_o.

(3) ROI generation: Let x_{tl} and y_{tl} represents as the minimal horizontal & vertical coordinates of ROI_o, wd and ht are the width and height of the bounding box of ROI_o. The finial ROI is a rectangle which is illustrated in Eq. (5) where p_x and p_y is the coordinate of the i^{th} I_b and d is equal to 100, that is huge enough to overlap the regions of fetal heart entirely.

$$ROI_t = \begin{cases} p_x = x_{tl} + wd + d \\ p_y = y_{tl} - ht - d \end{cases} \tag{5}$$

3. Segmentation

Medical image segmentation is a problem-posed question to resolve kinds of specific problem, furthermore, the specific task-related knowledges are required during the regularization process [8]. For example, the gray-level distribution, intensity gradient and textures are common used in fetal heart ultrasound image segmentation algorithm.

For achieving high accuracy and robustness results in the segmentation progress, there are several models have been proposed literately. The existed could be classified into four categories:

(1) The cluster-based method: These kinds of method assume that every single pixel as a sample and group of pixels fall into the identical issue which determines a subject-specific distribution. Afterwards, the 2D fetal heart ultrasound image is segmented by applying cluster-based algorithm. The cluster methods are heavily depended on initial clustering centers to keep the high efficiency [9, 10].

(2) The graph cut based algorithm: The algorithms transform the segmentation problem into a graph-cut problem between different correlated pixels, after that the segmentation curve is selected from the categorized of minimized energy in cut energy model. In addition, the accurate weights of the correlations between different pixels are difficult to construct, which leads to different segmentation problems such as under segmentation problem, over segmentation problem and so on [11, 12].

(3) Neural network-based system: It plays more and more important role and receives a range of prospects, which has been designed to execute quite a few tasks. However, it needs a lot of 603abeled dataset to train the network and output effects often give a rough result but not satisfactory segmentation in target distinct [13-15].

(4) The active contour-based technique: These techniques are generally relied on a curve being evolved from the initialized shape with image features such as gradient and curvature to fit the shape around the segmenting object. [16-18] Until now, it is a high effective algorithm that could be generally divided into region-based and edge-based models, respectively [19-21].

In this part, we will apply gradient vector flow (GVF) image segmentation approach to our fetal heart image to detect edges for handling boundary and region information. Section 3.1 and 3.2 describe the characteristic and benefits of active contour method and GVF algorithm [22-24].

3.1. Active Contour Method

Active contour method is first introduced by Kass et al. [25], it also known as snake model, that the contour divided minimize the contour-energy into the internal and external energy from the contour and the image respectively. The target of the internal energy is to keep the evolution curve smoothing and regularly, which is constructed from the first and second order derivatives. Besides that, the external energy is considered as the integral of different curve gradients which drives to form ROI boundary. When the contour meets minimum of energy, the deformation finally stops.

Recently, there are eight different deformable contour methods were reviewed by Lei which includes topology snake, GVF model, balloon snake model, area and length active contour model, geodesic active contour, distance snake, and a constrained optimization method in medical image segmentation field [26]. In their experiment part, five different medical images including MRI knee, blood cells, MRI brain, CT kidney,

UNIVERSIDAD DEL ZULIA
Serbiluz
Sistema de Servicios Bibliotecarios y de Información
Biblioteca Digital
Repositorio Académico

ultrasound pig heart are tested. Within given input images, different active contour algorithms have different characteristics, and in the ultrasound image field, the GVF model was determined to provide the best qualitative. Therefore, we will apply GVF snake model for segmenting the ultrasound fetal heart image.

3.2. Gradient Vector Flow

GVF is produced by a process that diffuses and smooths an input vector field and is usually used to create a vector field that points to object edges from a distance. In [27], Xu proposed the original GVF model. This paper first discussed the limitations of the original snake, and then it reported that external force field is irrotational which based on the contour points and the closest edge points in the contour points' normal direction. There is no external force pointing into the concavities inside due to the limits of deformation into boundary concavities. Therefore, the GVF model creates a novel external force field which is not entirely irrotational.

A new external force of GVF snake is constructed: F (v) = $(\alpha(x,y),\beta(x,y))$ and F(v) is achieved by the minimum the energy functional which is represented in Eq.(6):

$$E = \int\int \mu\left(\alpha_x^2 + \alpha_y^2 + \beta_x^2 + \beta_y^2\right) + |\nabla f|^2|F - \nabla f|^2 dxdy \tag{6}$$

In Eq. (6), an edge map is represented as f, a regularization parameter is illustrated as μ. Furthermore, the following Euler equations in (7) are needed for calculating the parameters of F and ∇^2 is represented as the Laplacian operator and $f_x = \frac{\partial f}{\partial x}$, $f_y = \frac{\partial f}{\partial y}$

$$\begin{cases} \mu\nabla^2\alpha - (\alpha - f_x)\left(f_x^2 + f_y^2\right) = 0 \\ \mu\nabla^2\beta - \left(\beta - f_y\right)\left(f_x^2 + f_y^2\right) = 0 \end{cases} \tag{7}$$

4. Experiment

4.1. Dataset

(a) (b)

Figure 3. The example of original (a) normal fetal heart image and (b) abnormal fetal heart image in echocardiogram datasets

The implementation of the proposed segmentation algorithm was applied by using ultrasound fetal heart echocardiogram datasets of 1727 images, that includes 1427 healthy images and 300 unhealthy images. Fig. 3 shows an example of normal and abnormal fetal heart image which will be applied in this section.

The population was ethnic Han with gestational age from 18-22 weeks. The images were collected through multi-center in China by using an Aloka 10, a Voluson E8-RAB4-8 with a 2- to 8-MHz transducer, UST-9130, with a 3- to 6- MHz transducer or a Philips iU-22, C5-1, and with a 1- to 5-MHz transducer. In addition, all the fetal heart images were collected by following the guidelines and standards of the American Society of Echocardiography [28–31].

The proposed automatic 2D ultrasound fetal heart segmentation algorithm was executed by using Python 3.6. All experiments were performed on a MacBook Pro laptop with 2.7 Ghz Intel Core i5 and 8GB memory.

4.2. Metrics and Parameters

In the first step of the proposed algorithm, the ROI generation would apply average precision rate (APR) and average recall rate (ARR) to calculate the effects.

$$APR = \frac{1}{N_T}\sum_{i=1}^{N_T}\left(N_i^{DR}/N_i^{D}\right) \tag{8}$$

UNIVERSIDAD DEL ZULIA
Serbiluz
Sistema de Servicios Bibliotecarios y de Información
Biblioteca Digital
Repositorio Académico

$$APR = \frac{1}{N_T}\sum_{i=1}^{N_T}\left(N_i^{DR}/N_i^{R}\right) \quad (9)$$

In Eq.(8) and (9), N_T is the total number of images, N_i^{DR} is the overlapped area between ROI and fetal heart area(manually selected), N_i^{D} is the size of ROI and N_i^{R} is the size of the fetal heart regions of ultrasound image i.

The performance of the proposed active contour-based image segmentation algorithm is validated by applying Dice similarity coefficient (DSC). The overlapped two image segmentation regions are measured by DSC, the first image D_1 segments manually and D_2 as the second image represents the segmentation results by applying proposed algorithm. Eq. (10) illustrated the formula of DSC

$$DSC(D_1, D_2) = \frac{|D_1 \cap D_2|}{|D_1 \cup D_2|} \quad (10)$$

4.3. ROI Generation

As we described in section 2, there are two steps in ROI generation, the first step is pre-processing for reducing noise and normalizing intensities, after that, the ROI generation is following which will generate fetal heart region.

1) Preprocessing.

There are several tasks in the preprocessing step, the first task aims to reduce the undesirable speckle noise, and after that, hypoechoic regions need to be normalized intensities to enhance the hypoechoic regions. Fig.4 illustrated the results of pre-processing step in normal and abnormal fetal heart image.

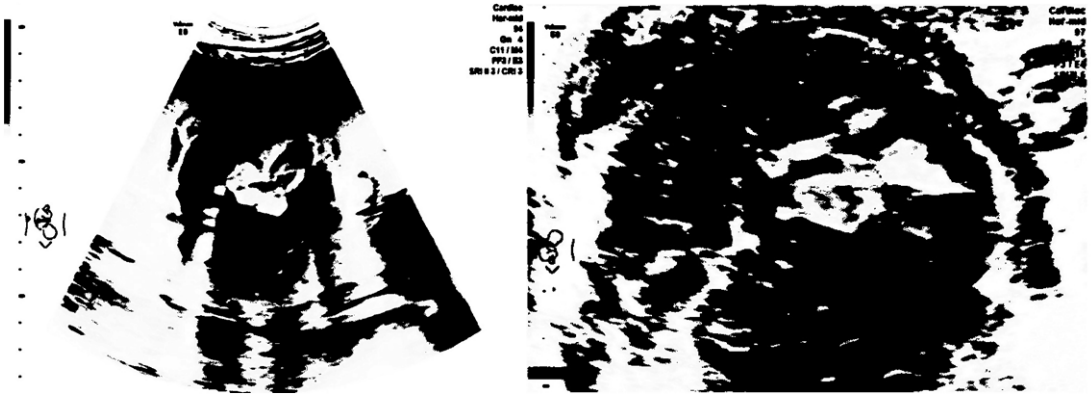

(a) (b)

Figure 4. The results of (a) normal fetal heart image and (b) abnormal fetal heart image after pre-processing

2) The ROI generation results.

(a) (b)

Figure 5. ROI generation of (a) normal fetal heart image and (b) abnormal fetal heart image

Fig.5 shows the exampled results of ROI generation of fetal heart images. As can be seen from it, we found that the proposed method could detect and locate the ROI of fetal heart image completely.

Table 1. Performance of ROI generation algorithms

	Types of Image	APR (%)	ARR
Metrics	Normal exampled image	90.39%	25.64
	Abnormal exampled image	90.26%	26.52

UNIVERSIDAD DEL ZULIA
Serbiluz
Sistema de Servicios Bibliotecarios y de Información
Biblioteca Digital
Repositorio Académico

Furthermore, the overall performances of the proposed ROI generation method is shown in Table 1. The APR of the proposed method in normal exampled images arrive 90.39%, and in abnormal exampled image achieve 90.26%.

4.4. Fetal Heart Image Segmentation Results

Table 2. Quantitative results for validating segmentation

Metrics	Types of image	DSC
	Normal exampled image	91.56%
	Abnormal exampled image	85.87%

In this part, we apply GVF algorithm to track the boundary from the ROI generated ultrasound fetal heart image, the result is shown in Fig.6 and Tab.2. As we found that, the proposed method can segment the fetal heart completely and it also keep high accuracy between manually and automatically segmented image.

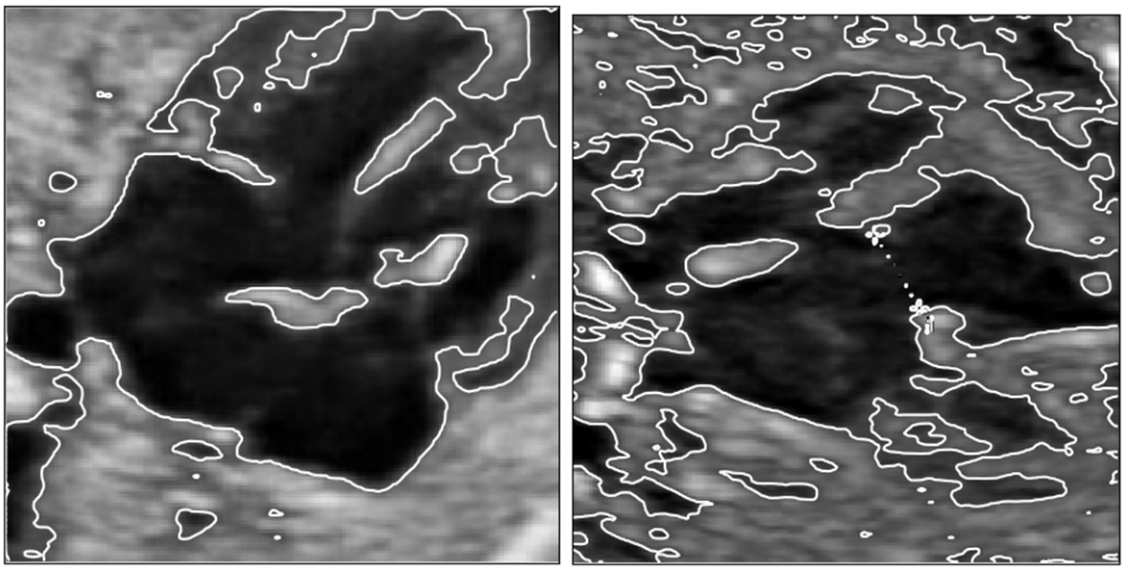

(a) (b)

Figure 6. Fetal heart image segmentation of (a) normal fetal heart image and (b) abnormal fetal heart image

5. Discussion and Conclusion

5.1. Discussion

Ultrasound imaging has been used in obstetric observation of the fetus and diagnosis of fetal diseases for more than half a century. The initial purpose of the ultrasound examination is only to determine fetal survival, gestational age and so on. Currently, it has become an indispensable diagnostic tool for diagnosing fetal abnormalities, and it is gained more insight into the ongoing development of the fetus. Therefore, with the rapid development of image technology, the fetal heart ultrasound image analysis approaches have been studies which includes image segmentation, detection, location and classification.

In our work, the active contour-based algorithm is applied, the pre-processing progress, ROI generation progress and the segmentation progress as three main characteristics plays an important role, the proposed algorithm segments the images completely with high accuracy. However, there still have several drawbacks in this field. First of all, this paper analyses the fetal ultrasound heart images, and focus on four chamber viewing planes, however, the left ventricular outflow tract viewing planes and three vessel viewing planes are also need to be analyzed. Secondly, the description of ultrasound videos of fetal heart needs to be improved, the content of each ultrasound video frame needs to be considered to predict cardiac phase. Finally, the labelled dataset of ultrasound fetal heart images is in short supply, the deep learning framework or AI algorithm has large potential prospect.

UNIVERSIDAD DEL ZULIA
Serbiluz
Sistema de Servicios Bibliotecarios y de Información
Biblioteca Digital
Repositorio Académico

5.2. Conclusion

In this paper, we propose an original automatic ultrasound fetal heart image segmentation algorithm. Firstly, the method is in the pre-processing stage to reduce noise and normalize intensities, after that, the ROI region is extracted, and then the GVF algorithm is applied in the step of segmentation progress to detect the edge of fetal heart regions. The experiments indicate that the proposed ROI generation and segmentation method keeps high accurate rate.

Besides the advantages of the proposed algorithm which described above, there are several open questions raised need to be considered in the future. Firstly, the orientation of the fetal heart is not analyzed, this is a significant question because the fetus relative to the direction of the propagation is still unknown. Secondly, congenital heart disease includes a large variety of interacting abnormalities, and it needs multi-dimensional analysis, therefore, the LVOT and 3V viewing plane should be considered to examine in the future.

Acknowledgement

This study is supported by the Beijing Key Laboratory of Maternal-Fetal Medicine in fetal heart disease (BZ0308); the Beijing Laboratory for Cardiovascular Precision Medicine (116211); the Beijing municipal science & technology commission reform and development programs(Z151100003915142); Cultivation of high level health technical personnel in Beijing health system (2015-3-409); the Beijing Municipal Administration of Hospitals Clinical medicine Development of special funding support (XMLX201604); the Beijing Municipal Science and Technology Commission (BJMSJY-160153); and the National Natural Science Foundation of China (61702027).

Reference

[1] Friedberg, M. K., Silverman, N. H., Moon-Grady, A. J., Tong, E., Nourse, J., Sorenson, B., Hornberger, L. K. (2009) "Prenatal Detection of Congenital Heart Disease", *Journal of Pediatrics*, 155(1), pp. 26-31.

[2] Bridge, C. P., Ioannou, C., & Noble, J. A. (2017) "Automated Annotation and Quantitative Description of Ultrasound Videos of the Fetal Heart", *Medical Image Analysis*, 36, pp. 147-161.

[3] Nageswari, C. S., & Prabha, K. H. (2018) Preserving the Border and Curvature of Fetal Heart Chambers through Tdywt Perspective Geometry Wrap Segmentation", *Multimedia Tools and Applications*, 77(8), pp.10235-10250

[4] Nageswari, C. S., & Helen Prabha, K. (2018) "Spatially Constrained Distance Regularized Level Set Evolution Method for Segmentation of Hydrops Fetalis from Ultrasound Fetal Heart Images", *Design Automation for Embedded Systems*, 22(1), pp. 45-64.

[5] Xian, M., Zhang, Y., & Cheng, H. D. (2015) "Fully Automatic Segmentation of Breast Ultrasound Images Based on Breast Characteristics in Space and Frequency Domains", *Pattern Recognition*, 48(2), pp.485-497.

[6] Doane, D. P., & Seward, L. E. (2011) "Measuring Skewness: A Forgotten Statistic", *Journal of Statistic Education*, 19(2), pp. 1-18.

[7] Gonzalez R, Woods R. (1992) "*Chap.2. Digital image processing*", *Addision-Wesley Publishing Company.*

[8] Chittajallu, D. R., Brunner, G., Kurkure, U., Yalamanchili, R. P., & Kakadiaris, I. A. (2009) "Fuzzy-Cut: A Knowledge-Driven Graph-Based Method for Medical Image Segmentation", *Proceedings of IEEE CVPR*, (6), pp. 715-722.

[9] Ribbens, A., Hermans, J., Maes, F., Vandermeulen, D., & Suetens, P. (2013) "Unsupervised Segmentation Clustering, and Groupwise Registration of Heterogeneous Populations of Brain MR Image", *IEEE Transactions on Medical Imaging*, 33(2), pp. 201-224.

[10] Gong, M., Liang, Y., Shi, J., Ma, W., & Ma, J. (2012) "Fuzzy C-Means Clustering with Local Information and Kernel Metric for Image Segmentation", *IEEE Transactions on Image Processing*, 22(2), pp. 573-584.

[11] Kuo, J. W., Mamou, J., Aristizábal, O., Zhao, X., Ketterling, J. A., & Wang, Y. (2015) "Nested Graph Cut for Automatic Segmentation of High-Frequency Ultrasound Images of the Mouse Embryo", *IEEE Transaction on Medical Imaging*, 35 (2), pp. 427-441.

[12] Li, G., Chen, X., Shi, F., Zhu, W., Tian, J., & Xiang, D. (2015) "Automatic Liver Segmentation Based on Shape Constraints and Deformable Graph Cut in CT Images", *IEEE Transactions on Image Processing*, 24(12), pp. 5315-5329.

[13] Long, J., Shelhamer, E., & Darrell, T. (2015) "Fully Convolutional Networks for Semantic Segmentation", *IEEE Transactions on Pattern Analysis and Machine Intelligence*, 39 (4), pp. 3431-3440.

[14] He, K., Gkioxari, G., Dollár, P., & Girshick, R. (2017) "Mask R-CNN", *Proceedings of the IEEE International Conference on Computer Vision*, pp. 2961-2969.

UNIVERSIDAD DEL ZULIA
Serbiluz
Sistema de Servicios Bibliotecarios y de Información
Biblioteca Digital
Repositorio Académico

[15] Ronneberger, O., Fischer, P., & Brox, T. (2015) "U-Net: Convolutional Networks for Biomedical Image Segmentation", *Proceedings of Medical Image Computing and Computer-Assisted Intervention*, pp. 234–241.
[16] Li, C., Huang, R., Ding, Z., Gatenby, J. C., Metaxas, D. N., & Gore, J. C. (2011) "A Level Set Method for Image Segmentation in the Presence of Intensity Inhomogeneities with Application to MRI", *IEEE Transactions on Image Processing*, 20 (7), pp. 2007-2016.
[17] Yang, X., Gao, X., Tao, D., Li, X., & Li, J. (2014) "An Efficient MRF Embedded Level Set Method for Image Segmentation", *IEEE Transactions on Image Processing*, 24 (7), pp. 9–21.
[18] Zhang, K., Zhang, L., Lam, K. M., & Zhang, D. (2015) "A Level Set Approach to Image Segmentation with Intensity Inhomogeneity", *IEEE Transaction on Cybernetics*, 46 (2), pp. 546–557.
[19] Wang, L., Chang, Y., Wang, H., Wu, Z., Pu, J., & Yang, X. (2017) "An Active Contour Model Based on Local Fitted Images for Image Segmentation", *Information Science*, 418, pp. 61-73.
[20] Zhang, K., Song, H., & Zhang, L. (2010) "Active Contours Driven by Local Image Fitting Energy", *Pattern Recognition*, 43 (4), pp. 1199–1206.
[21] Wang, H., Huang, T. Z., Xu, Z., & Wang, Y. (2016) "A Two-Stage Image Segmentation via Global and Local Region Active Contours", *Neurocomputing*, 205: 130–140.
[22] Zhou, S., Wang, J., Zhang, M., Cai, Q., & Gong, Y. (2017) "Correntropy-Based Level Set Method for Medical Image Segmentation and Bias Correction", *Neurocomputing*, 234(2017), pp. 216–229.
[23] Yang, X., Gao, X., Tao, D., & Li, X. (2014) "Improving Level Set Method for Fast Auroral Oval Segmentation", *IEEE Transactions on Image Processing*, 23 (7), pp. 2854-2865.
[24] Yang, X., Gao, X., Li, J., & Han, B. (2014) "A Shape-Initialized and Intensity-Adaptive Level Set Method for Auroral Oval Segmentation", *Information Science*, 277 (2014), pp. 794–807.
[25] Kass, M., Witkin, A., & Terzopoulos, D. (1988) "Snakes: active contour model", *International Journal of Computer Vision*, 1(4), pp. 321-331.
[26] He, L., Peng, Z., Everding, B., Wang, X., Han, C. Y., Weiss, K. L., & Wee, W. G. (2008) "A Comparative Study of Deformable Contour Methods on Medical Image Segmentation", *Image and Vision Computing*, 26(2008), pp. 141-163.
[27] Xu, C., & Prince, J. L. (1998) "Snake, Shapes and Gradient Vector Flow", *IEEE Transaction on Image Processing*, 7(3), pp. 359-369.
[28] Gu, X., Zhu, H., Zhang, Y., Han, J., Zhang, H., Liu, Y., Weng, Z. (2019) "Quantile Score: A New Reference System for Quantitative Fetal Echocardiography Based on a Large Multicenter Study", *Journal of the American Society of Echocardiography*, 32(2), pp. 296-302.
[29] Rychik, J., Ayres, N., Cuneo, B., Gotteiner, N., Hornberger, L., Spevak, P. J., & Van Der Veld, M. (2004) "American Society of Echocardiography Guidelines and Standards for Performance of the Fetal Echocardiogram", *Journal of the American Society of Echocardiography*, 17(7), pp. 803-810.
[30] Donofrio, M. T., Moon-Grady, A. J., Hornberger, L. K., Copel, J. A., Sklansky, M. S., Abuhamad, A., Lacey, S. (2014) "Diagnosis and Treatment of Fetal Cardiac Disease a Scientific Statement from the American Heart Association", *Circulation*, (129)21, pp. 2183-2242.
[31] Shapiro, I., Degani, S., Leibovitz, Z., Ohel, G., Tal, Y., & Abinader, E. G. (1998) "Fetal Cardiac Measurements Derived by Transvaginal and Transabdominal Cross-Sectional Echocardiography from 14 Weeks of Gestation to Term", *Ultrasound in Obstetrics & Gynecology*, 12(6), pp. 404-418.
[32] Sampath, S., & Sivaraj, N. (2014) "Fuzzy Connectedness Based Segmentation of Fetal Heart from Clinical Ultrasound Images", *Advanced Computing, Networking and Informatics*, 1, pp. 329-337.
[33] Smistad, E., & Østvik, A. (2017) "2D Left Ventricle Segmentation Using Deep Learning", *IEEE International Ultrasonic Symposium*, pp. 1-4.
[34] Wang B., Chen L., Cheng J. (2018) "New Result on Maximum Entropy Threshold Image Segmentation Based on P System", *OPTIK*, 163, pp. 81-85.